



Comparative Study on Copper Oxide Nanocrystals Synthesized by Two Precipitation Methods



CrossMark

Maroof A. Hegazy,^a, Hayat H. El-Agamy,^{b,*}

^aNano Technology Unit, Solar and Space Research Department, National Research Institute of Astronomy and Geophysics (Nano NRIAG), 11421 Helwan, Cairo, Egypt

^bNuclear Materials Authority (NAM), El Katameya, Cairo, Egypt

Abstract

Copper oxide (CuO) nanostructures have attracted a lot of interest in recent years due to their interesting properties. In this study, preparation CuO nanostructures through the chemical reduction of copper sulfate with acetic acid. In our synthesis route, starch was added and worked both as a size and shape controller. The synthesized nanostructures were characterized by X-ray diffraction (XRD), Fourier transform infrared spectroscopy (FTIR) and transmittance electron microscope (TEM). The average particle diameters were determined by the Debye-Scherrer equation and Analysis by Thermogravimetric analysis (TGA), BET.

Keywords: Nano copper oxide; Starch; Precipitation method; Acetic acid.

1. Introduction

The controlled fabrication of nanoparticles has prompted nanotechnology into one of today's most auspicious and prevalent fields of scientific research [1]. Possibility future advancement presupposes the ability to synthesis nanomaterials in a numerous and controlled manner [2-8]. Currently, there is an increasing interest to prepare CuO is one of potential p-type semiconductors and acquires significant attentions due to its excellent optical, electrical, magnetic properties sensing, surface properties and physical properties such as electron correlation effects, spin dynamics and high temperature superconductivity [9-11]. CuO have narrow band gap of 1.2 eV extensively used in diverse applications such as catalysis [12,13], solar energy conversion [14], gas sensor [15] and field emission [16].

However, these novel properties can be amended by prepare in CuO nanostructures that shown excellent performance comparing to bulk counterpart. Various nanostructures of CuO are synthesized in form of nanowire, nanorod, nanoneedle, nano-flower and nanoparticle. In the past decades, various methods have been proposed to produce CuO nanoparticles with different sizes and shapes such as thermal oxidation [17], sonochemical [18], combustion [19] and quick-precipitation [20,21].

Among these processes, a simple quick precipitation is usually distinguished, because this method is simple, cost-effective and efficient, and it can improve size and size dispersion control by optimizing the experimental factors, for example the molar ratio of the stabilizer with the precursor salt and the fraction of reducing agent with the precursor salt [22-24]. The rate of growth of the nanoparticles count on diverse variables, including the concentration of metal ions, the type of reductant, pH, temperature and time [25]. In the present work, the main aim is to research the effect of capping agent on structural properties of CuO nanostructures synthesized via precipitation method. Copper nitrate and starch was chosen as capping agent. The as-prepared precipitates were characterized using by scanning electron microscopy, X-ray diffractometer and FTIR Spectroscopy.

2. Experimental work

2.1. Materials

All the reagents and solvents used in this research were of analytical grade. Copper sulfate pentahydrate (CuSO₄·5H₂O) was used as the copper ion precursor. Similarly, acetic acid (as anti-oxidant), potassium hydroxide (for adjusting the pH) and starch (as capping agent) were purchased from MERCK, Germany.

*Corresponding author e-mail: hayatrock97@hotmail.com; (Hayat H. El-Agamy).

Receive Date: 30 December 2020, Accept Date: 15 January 2021

DOI: 10.21608/EJCHEM.2021.55876.3190

©2021 National Information and Documentation Center (NIDOC)

2.2. Analytical methods

1. The functional groups and chemical structure were estimated by FT-IR spectroscopy using a Perkin-Elmer FT-IR-2000 spectrometer, US.
2. Powder X-ray measurement was performed on a Rigaku Ultima IV diffractometer with Cu K α radiation at 40 kV and 40 mA in the range of $2\theta=0-80$ and the scanning rate was $5^\circ/\text{min}$.
3. The FETEM images were recorded using the Field Emission Transmission Electron Micrographs (FETEM), brand-JEOL and model-JEM-2100F.
4. The average particle size was studied from the TEM images using softwares such as Image J and Origin.

2.3. Synthesis methods

2.3.1. CuO nanoparticles were synthesized by the chemical precipitation method

Precipitation method I: At the first dissolving 2.5 g of copper sulfate pentahydrate ($\text{CuSO}_4 \cdot 5\text{H}_2\text{O}$) in 300 ml of distilled water and then added 3 ml of glacial acetic acid in a volumetric flask at high mixing speed. At The second dissolving 1 M of sodium hydroxide in 100 ml of distilled water was added gradually dropped into the solution under magnetic stirring at 80°C , until the mixture's pH reached the value of 6, the point at which a great quantity of black precipitation was simultaneously created then the precipitation was centrifuged and washed with water. Finally, the black powder was calcined at 500°C for 2 h and then milled.

2.3.2. Precipitation method II - the preparation method starts with addition of 2.5 g copper (II) sulfate

Pentahydrate solution into 100 mL of starch (1 %) solution with vigorous stirring for 30 min. and then added 3ml of glacial acetic acid in a volumetric flask at high mixing speed. At The second dissolving 1 M of sodium hydroxide in 100 ml of distilled water was added gradually dropped into the solution under magnetic stirring at 80°C , until the mixture's pH reached the value of 6, the point at which a great quantity of black precipitation was simultaneously created then the precipitation was centrifuged and washed with water. Finally, the black powder was calcined at 500°C for 2 h and then milled.

3. Results and discussion

3.1. Structural properties

XRD pattern (Fig. 1a) of the products formed is identical to the single-phase CuO with a monoclinic structure and the diffraction data are in good agreement with JCPDS card of CuO (JCPDS 80-1268). The

broadening of the peaks indicates the small size of the products. Actually, the average size of the CuO nanoparticles is estimated to be 10 nm according to the Scherrer equation [12].

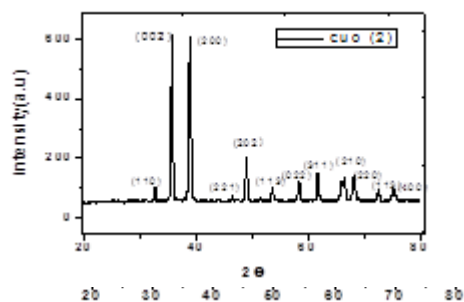


Fig. 1. b shows the XRD spectrum of CuO nanoparticles.

X-ray diffraction (XRD) pattern higher intensity peaks at 38.9° , 35.6° and 48.9° which correspond to the atomic planes (200), (002) and (202) respectively were observed in the diffraction. In this study the average crystallite size of the highest peak (38.9°), is estimated about 42nm by Scherrer's Morphologies of CuO nanoparticles are presented in Figs. 2a and 2b, as obtained by TEM.

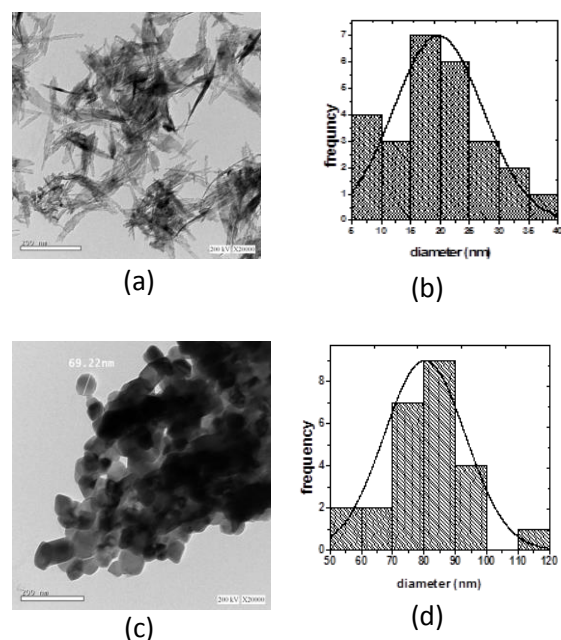


Fig. 2. (a) TEM image of CuO nanoneedles, (b) Statistical histogram of average particle size of the nanoneedles (c) TEM image of CuO nanoparticles and (d) Statistical histogram of average particle size of the nanoparticles

Figure 2(a), shows that the CuO nanoparticles had nanoneedle shapes, whose diametric average is more than 10 nm. The particle-size distribution histogram of CuO nanoparticles (Figure 2b) indicated that the average diameter of nanoparticles counted from the TEM image is about 20 nm.

Figure 2c shows that the CuO nanoparticles had spherical shapes. An agglomeration of nanoscale particles is clearly observed, showing a uniform distribution of particle size and a homogeneous morphology. The particle-size distribution histogram of CuO nanoparticles (Figure 2b) indicated that the average diameter of nanoparticles counted from the TEM image is about 70 nm.

3.2. Fourier transform infrared spectroscopy analysis

Investigated the pure CuO (1) and CuO (2) nanoparticles annealed at 500 °C were analyzed by FT-IR analysis as shown in Fig. 3 and 4. The bands between 800–400 cm⁻¹ represent the presence of metal oxygen [20–22]. In the present investigation the low frequency region 400–700 cm⁻¹ assigned the vibrational properties of CuO nanostructures corresponds to 498 cm⁻¹ has been Cu–O monoclinic phase of the pure CuO(1) nanoparticles and also, 534 cm⁻¹ has been Cu–O monoclinic phase CuO(2) nanoparticles.

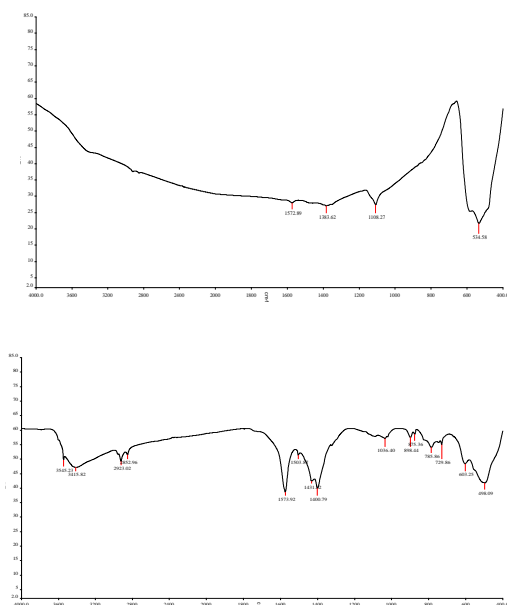


Fig. 3. FTIR spectrum of CuO nanoneedles and (b) FTIR spectrum of CuO of CuO nanoparticles

The FTIR spectrum of the sample is taken and shown in figure 3. The spectrum shows the following characteristics: the peaks at 498.09 cm⁻¹ (Cu–O symmetric stretching) and at 603.24 cm⁻¹ (Cu–O wagging) imply the presence of metal-oxide group in the sample. The vibration peak 3415 cm⁻¹ indicates the presence of hydroxide group in the sample. This may be due to the water attached to the surface of the CuO nano-particles, which is also one of the products of the reaction and can be removed by further

heating. The metal–oxygen bond is observed at 1400 cm⁻¹ (M–O rocking in plane) and at 1573.92 cm⁻¹ (M–O rocking out of plane) indicate the formation of CuO from copper sulphate [24].

3.3. Thermogravimetric analysis

Thermogravimetric analysis (Figure 4) revealed that nano copper oxide with starch degraded in a multiple steps process. Degradation of starts at about 64 oC till approximately 160 oC.

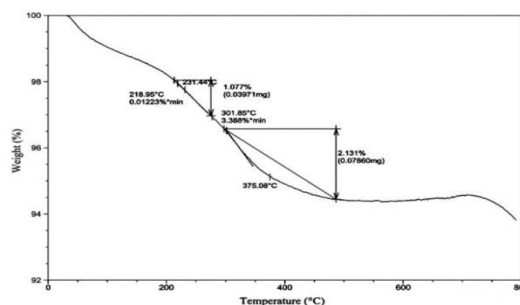


Fig. 4. TGA curve obtained for CuO with starch

This loss in weight could be due to the presence of moisture in the sample. A less marked decomposition starts at about 218 oC while the greatest degradation takes in the range of 301- 470oC approximately with most decomposition temperature of around 375.8oC.

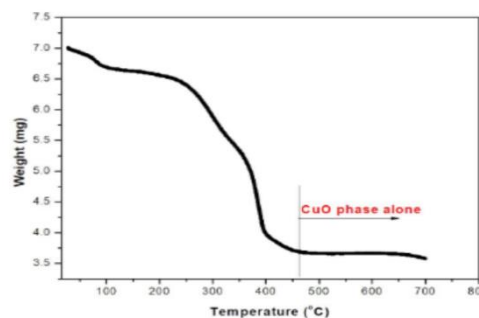


Fig. 5. TGA curve obtained for CuO without starch

From the figure (4), it can be seen that the sample nano copper oxide without starch heated up to 94.5 °C undergoes a total weight loss of 0.304 mg (4.34 %), which is attributed to the liberation of moisture adsorbed on the surface of the sample. Further 0.240 mg loss up to 240.6 °C is satisfied by elimination of volatile components present in the sample. The decomposition step between 239.6 °C and 464 °C is generally ascribed to the elimination of carbon group compounds present in the sample.

4. Conclusions

In this work CuO nanostructures were synthesized by precipitation method without and with using starch lead to change in the particle size and shape of nanostructure lead to the great advancement in their applications such as catalysis and photoactivated energy conversion.

5. References

- [1] Shenmar R., Norsten V. B., Rotello V. M., Polymer-mediated nanoparticle assembly: structural control and applications, *Advanced Material*, 6, 657-669 (2005).
- [2] Balzani V., Credi A., Venturi M., The Bottom-Up Approach to Molecular- Level Devices and Machines, *Chemistry A European Journal*, 8, 5524-5532, (2002).
- [3] Ezzat H. A., Gomaa I., Gawad A. A., Osman O., Mahmoud A. A., Sleim M., Elhaes H., Ibrahim M. A., Semiempirical Molecular Modeling Analyses for Graphene/Nickel Oxide Nanocomposite, *Letters in Applied NanoBioScience*, 9, 1459-1466, (2020).
- [4] Badry R., Ibrahim A., Gamal F., Shehata D., Ezzat H., Elhaes H., Ibrahim M., Electronic Properties of Polyvinyl Alcohol/ TiO₂/SiO₂ Nanocomposites, *Biointerface Research in Applied Chemistry*, 10, 6427- 6435 (2020).
- [5] Ezzat H. A., Hegazy M. A., Nada N. A., Ibrahim M. A., Effect of nano metal oxides on the electronic properties of cellulose, chitosan and sodium alginate, *Biointerface Research in Applied Chemistry*, 9, 4143- 4149 (2019).
- [6] Ezzat H. A., Hegazy M. A., Nada N. A., Osman O., Ibrahim M. A., Application of natural polymers enhanced with ZnO and CuO as humidity sensor, *NRIAG Journal of Astronomy and Geophysics*, 9, 586 - 597 (2020).
- [7] Elhaes H., Ezzat H., Badry R., Yahia I.S., Zahran H.Y., Ibrahim M.A., The Interaction Between Carbon Nanotube Decorated with CuO and ZnO and Hydrogen, *Sensor Letter*, 16, 445 – 453 (2018).
- [8] Elhaes H., Ezzat H., Morsy M., El-Khodary S.A., Yahia I.S., Zahran H.Y., Ibrahim M.A., PVC/ZnO nano-composite as gas sensor for natural gas, *Sensor Letter*, 16, 513-516 (2018).
- [9] Lambert S., Cellier C., Gaigneaux E. M., Pirard J. P., Heinrichs B., Ag/SiO₂, Cu/SiO₂ and Pd/SiO₂ cogelled xerogel catalysts for benzene combustion: relationships between operating synthesis variables and catalytic activity, *Catalysis Communications*, 8, 1244-1248 (2007).
- [10] Zhang H., Zhu Q., Zhang Y., Wang Y., Zhao L., Yu B., One- Pot Synthesis and Hierarchical Assembly of Hollow Cu₂O Microspheres with Nanocrystals- Composed Porous Multishell and Their Gas- Sensing Properties, *Advanced Functional Materials*, 17, 2766-2771 (2007).
- [11] Akintelu S. A., Folorunso A. S., Folorunso F.A., Oyebamiji A. K., Green synthesis of copper oxide nanoparticles for biomedical application and environmental remediation, *Heliyon*, 6, e04508 (2020)
- [12] Yan J. C., Tianyi W., Liu M. Y., Yuan Zh., Synthesis of porous hematite nanorods loaded with CuO nanocrystals as catalysts for CO oxidation, *Journal of Natural Gas Chemistry*, 20, 669-676 (2011).
- [13] Kaneshiro J., Gaillard N., Rocheleau R., Miller E., Advances in copper-chalcopyrite thin films for solar energy conversion, *Solar Energy Materials and Solar Cells*, 94, 12-16 (2010).
- [14] Méndez-Medrano M. G., Kowalska E., Lehoux A., Herissan A., Ohtani B., Bahena D., Remita H., Surface Modification of TiO₂ with Ag Nanoparticles and CuO Nanoclusters for Application in Photocatalysis, *The Journal of Physical Chemistry C*, 120, 5143-5154 (2016).
- [15] Zhang Y., He X., Li J., Zhang H., Gao X., Gas-sensing properties of hollow and hierarchical copper oxide microspheres, *Sensors and Actuators B: Chemical*, 128, 293-298 (2007).
- [16] Zhang J., Liu J., Peng Q., Wang X., Li Y., Nearly Monodisperse Cu₂O and CuO Nanospheres: Preparation and Applications for Sensitive Gas Sensors, *Chemistry of Materials*, 18, 867-871 (2006).
- [17] Alajlani Y., Placido F., Chu H. O., De Bold R., Fleming L., Gibson D., Characterisation of Cu₂O/CuO thin films produced by plasma-assisted DC sputtering for solar cell application, *Thin Solid Films*, 642, 45-50 (2017).
- [18] Bohr R. H., Chun S. Y., Dau C. W., Tan J. T., Sung J., Field emission studies of amorphous carbon deposited on copper nanowires grown by cathodic arc plasma deposition, *New Carbon Materials*, 24, 97-101 (2009).
- [19] Dang T. M. D., Le T. T. T., Blanc E. F., Dang M. C., The influence of solvents and surfactants on the preparation of copper nanoparticles by a chemical reduction method, *Advances in Natural Sciences: Nanoscience and Nanotechnology*, 2, 1-7 (2011) .
- [20] Han K. N., Kim N. S., Challenges and Opportunities in Direct Write Technology Using Nano-metal Particles, *KONA Powder Particle Journal*, 27, 73-83 (2009).
- [21] Zhu J.W., Li D., Yang X.J., Lu L.D., Wang X., Highly dispersed CuO nanoparticles prepared by a novel quick-precipitation method, *Materials Letters*, 58, 3324-3327 (2004).

-
- [22] Dalawai S. P. , Kumar S., Aly M. A. S., Khan Md. Z. H., Xing R., Vasambekar P. N., Liu Sh., A review of spinel-type of ferrite thick film technology: fabrication and application, *Journal of Materials Science: Materials in Electronics*, 30, 7752–7779 (2019).
- [23] Hammad T.M., Salem J.K., Harrison R.G., Binding agent affect on the structural and optical properties of ZnO nanoparticles, *Reviews on Advanced Materials Science*, 22, 74-81 (2009).
- [24] Basith M., Vijaya J. J., Kennedy L. J., Bououdina M., Structural, optical and room-temperature ferromagnetic properties of Fe-doped CuO nanostructures, *Physica E: Low-dimensional Systems and Nanostructures*, 53, 193-199 (2013).
- [25] Kumar I., Ranjan P., Quaff A. R., Cost-effective synthesis and characterization of CuO NPs as a nanosize adsorbent for As (III) remediation in synthetic arsenic-contaminated water, *Journal of Environmental Health Science and Engineering*, 1-10 (2020)